RSC Advances

PAPER

View Article Online
View Journal | View Issue

Cite this: *RSC Adv.*, 2024, **14**, 4645

Enhancing the water permeability of composite NF membranes through the incorporation of organic ions in the aqueous phase

Shuai Zhou, [ab] Huifen Tan,[b] Keke Chen,[b] Xin Cheng, [b] Xiaojuan Huang[ab] and Congjie Gao*[ac]

Received 23rd July 2023
Accepted 7th January 2024

DOI: 10.1039/d3ra04972h

rsc.li/rsc-advances

Composite nanofiltration (NF) membranes prepared using interfacial polymerization (IP) have gained significant attention in the field of wastewater treatment. In this study, sodium camphor sulfonate (CSA-Na) and tetraethylammonium chloride (TEAC) were employed as aqueous phase additives to regulate the diffusion of piperazine (PIP) molecules through electrostatic interactions. The dissociated CSA-Na and TEAC in the aqueous solution formed an organic structure at a certain concentration, restricting the interfacial transport behavior of PIP monomers. The results show that when the content of CSA-Na is 2% w/v, TEAC is 3.9% w/v, that is, the material dosage ratio is 1 : 3, and the NF membrane shows the best performance, with a water flux of 55.61 L m^{-2} h^{-1} (test pressure is 0.5 MPa), and $MgSO_4$ rejection rate of more than 98%.

1 Introduction

At present, the issues of resources and the environment are indeed becoming increasingly serious.[1,2] One key measure to alleviate the shortage and pollution of water resources is the use of membrane separation technology. Among the various membrane types, the nanofiltration (NF) membrane stands out as a pressure-driven membrane developed based on reverse osmosis separation technology. The NF membrane has a pore size ranging between 0.5–200 nm and exhibits a rejection rate of over 90% for neutral molecules with a molecular weight greater than 200 Da[3,4]. Due to this unique separation characteristic, NF membranes find frequent applications in various fields, including wastewater treatment, medicine, food, and desalination.[5–7]

Thin film composite (TFC) membranes, prepared using interfacial polymerization (IP),[8,9] have emerged as a superior alternative to asymmetric acetate cellulose membranes that were previously widely used in commercial production.[10] A typical TFC membrane consists of two main components. The first component is the support membrane, typically an ultrafiltration membrane, which serves as the medium for the IP reaction. The second component is the separation function layer, situated on top of the support membrane. This layer is formed through the polyreaction of highly reactive monomers at the interface between the aqueous and organic phases.[11–14] It is important to note that modification of both the support membrane and the separation layer can significantly impact the structure and performance of the TFC membrane. As a result, each layer of the TFC membrane fabricated *via* the IP process can be optimized semi-independently to achieve optimal separation performance.[15]

The adjustment process of IP in TFC membranes can be divided into two main parts: modification of the base membrane and optimization of both the aqueous and organic phases. Various approaches can be employed to manipulate the IP process parameters, post-treatment methods, introduce additives, and explore new monomers.[16–20] Among these approaches, the addition of suitable additives to the aqueous and organic phases has been proven to be a simple and effective method for optimizing TFC membrane performance. It achieves this by modulating the diffusion and reaction of monomers during the IP process.[21]

The incorporation of nanoparticles into the polyamide layer, for example, can introduce additional water molecule channels, leading to improved permeation flux.[22] Furthermore, this approach can help overcome the "trade-off" effect between solvent permeability and solute selectivity.[23–25] Wei *et al.*[26] prepared polyamide thin film nanocomposite nanofiltration membranes by incorporation of aminated titanium dioxide (APTES-TiO_2), resulting in excellent monovalent/divalent salts separation performance. Additionally, the use of aqueous polymer additives can also influence the IP process. Tan *et al.*[27] added polyvinyl alcohol (PVA) to the aqueous phase, which inhibited the diffusion rate of monomer molecules through hydrogen bonding and increased the viscosity of the solution.

[a]*Second Institute of Oceanography of the State Oceanic Administration, Hangzhou 310012, China. E-mail: gaocj@zjut.edu.cn*

[b]*Bluestar (Hangzhou) Membrane Industries Co., Ltd, No. 602 Shunfeng Road, Linping District, Hangzhou, China, 311100*

[c]*Zhejiang University of Technology, Hangzhou 310014, China*

Consequently, NF membranes with higher throughput and separation performance were obtained. Similarly, the selection of specific small molecule additives in the aqueous phase can also lead to improved membrane performance. Sun *et al.*[28] added sodium bicarbonate to the aqueous solution, which reacted with hydrochloric acid produced during IP. This reaction resulted in gas formation (CO_2), loosening the membrane structure and significantly improving the flux. Zhu *et al.* [29] incorporated glycerol into the aqueous solution, increasing its viscosity and inhibiting the diffusion of piperazine. This adjustment led to the formation of NF membranes with a linearly adjustable thickness ranging from 32.3 nm to 5.6 nm.

Overall, the exploitation and utilization of additives in the aqueous phase have emerged as a simple and effective approach for optimizing the performance of separation membranes.

Currently, significant research efforts are dedicated to incorporating additives into the aqueous and oil phases to enhance the overall performance of TFC films. However, the theoretical understanding of these effects is still lacking in maturity.[21] Traditional aqueous additives have been shown to improve the performance of TFC membranes by modulating monomer diffusion and modifying IP. However, there have been limited studies on the interaction between different types of additives.

In this particular study, the researchers focused on introducing organic ions in the aqueous phase to investigate the impact of electrostatic interactions between organic anionic and organic cationic ions on the IP reaction. By studying the effects of these interactions, the researchers aimed to gain a better understanding of how additive interactions influence the overall performance of TFC membranes.

Due to the limited solubility of acyl chloride monomers in the aqueous solution, the polymerization in IP predominantly occurs through the diffusion of amine monomers from the aqueous phase to the organic side of the interface. In this study, sodium camphor sulfonate (CSA-Na) and tetraethylammonium chloride (TEAC) were utilized as additives in the aqueous phase to modulate the diffusion behavior of PIP molecules during the IP process. This modulation was achieved through the electrostatic interaction between sulfonic acid ions (negatively charged) from CSA-Na and ammonium ions (positively charged) from TEAC in the aqueous solution.

CSA-Na is a derivative of camphor, a bicyclic monoterpene ketone, known for its antibacterial, deworming, anti-inflammatory, and analgesic properties.[30] When dissolved in water, CSA-Na exhibits a negative charge due to the ionization of the sulfonic acid group. On the other hand, TEAC is a quaternary ammonium salt with positively charged nitrogen atoms. When dissolved in water, TEAC forms ionic bonds and becomes positively charged. The focus of this research paper is centered around examining the effects of electrostatic interactions between anions (CSA-Na) and cations (TEAC) on the diffusion of PIP molecules and the subsequent fabrication of NF membranes. Besides, the effect of additional PVA in the aqueous phase on the membrane performance was investigated. It is hoped that the PVA can remarkably increase the diffusion resistance of the PIP,[31] so as to create an ideal aqueous phase environment for the monomer.

2 Experimental

2.1 Material

Polysulfone (PSf) substrates were provided by Hangzhou Water Treatment Technology Development Center (China).

Polyvinyl alcohol (PVA), sodium camphor sulfonate (CSA-Na), tetraethylammonium chloride (TEAC), piperazine (PIP), trimesoyl chloride (TMC), magnesium sulfate ($MgSO_4$), sodium chloride (NaCl) are analytically pure, purchased from Aladdin Reagent (China) Co., LTD. The deionized water is obtained through the combination of reverse osmosis (RO) and electrodeionization (EDI) treatment.

2.2 Interfacial polymerization of polyamide membranes

PSf substrates (molecular weight cut off is 50 000) with flat surface and no crease were selected and fixed with a polytetrafluoroethylene frame. Prior to the membrane formation process, the PSf substrates were kept in deionized water. The ambient temperature was 25 ± 1 °C.

As shown in Fig. 1, the initial step involved immersing the PSf substrate in 80 g aqueous solution containing PIP and PVA for a duration of 1 minute. Afterward, the substrate was allowed to air dry until no visible liquid droplets were present on the surface. Next, 20 g Isopar L solution of TMC, with a concentration of 0.1 g L^{-1}, was poured onto the PSf substrate for 20 seconds. Excess solution was carefully removed from the substrate. Finally, the reacted membrane was placed in an oven (DHG9140A, Shanghai Bluepard Instruments Co., Ltd) and heat-treated at a temperature of 100 °C for a duration of 3 minutes. This step helps in the further cross-linking and stabilization of the membrane structure. Finally, the prepared nanofiltration membrane samples were placed in deionized water and soaked for over 12 hours before being left to await testing.

In the aqueous phase solution, a mixture of CSA-Na at a concentration of 2% w/v and TEAC at varying concentrations ranging from 0% to 6.5% w/v was incorporated. The resulting NF membranes, prepared with different TEAC concentrations, were named Mx, with the value of *x* representing different types of membranes. The NF membrane that was prepared without the addition of TEAC was denoted as M0. The specific types and concentrations of additives used in the aqueous phase are summarized in the table below (Table 1):

2.3 Characterization

The surface morphology of the polyamide NF membrane was characterized using field emission scanning electron microscopy (FESEM,S-4800, Hitachi, Japan). Prior to observation, the membrane was cleaned and dried in a constant temperature oven. A suitable membrane size was selected to create a sample, which was then sputtered with gold. This process allows for enhanced imaging of the membrane surface using FESEM.

The surface functional groups of the NF membrane were analyzed using Attenuated Total Reflection Fourier Transform Infrared Spectroscopy (ATR-FTIR, S-4800, Hitachi, Japan). Before conducting the analysis, a background scan was performed using air as the reference, within a scanning range of

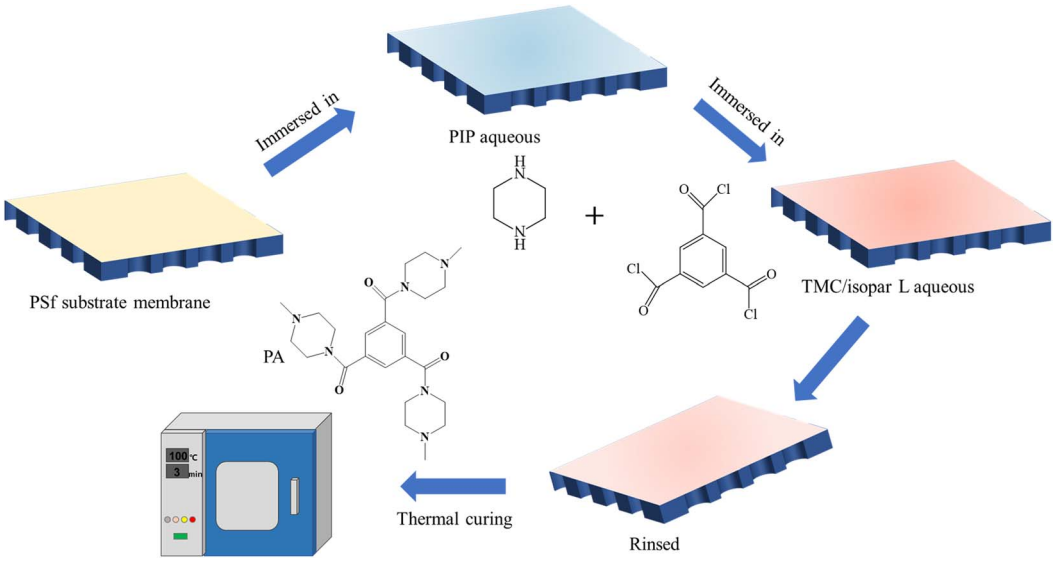

Fig. 1 Schematic fabrication of high flux NF membranes.

Table 1 The types of membrane and aqueous phase additives

Membrane	PIP (%)	PVA (%)	CSA-Na (%)	TEAC (%)
M0	0.15	0.1	2	0
M1	0.15	0.1	2	1.3
M2	0.15	0.1	2	2.6
M3	0.15	0.1	2	3.9
M4	0.15	0.1	2	5.2
M5	0.15	0.1	2	6.5
PA-0	0.15	0.1	0	0
PA-C	0.15	0.1	2	0
PA-T	0.15	0.1	0	1.3
PA-CT	0.15	0.1	2	1.3

500–4000 cm^{-1}. ATR-FTIR spectroscopy enables the identification and quantification of functional groups present on the membrane surface.

Atomic force microscopy (AFM, Bruker Dimension icon, Germany) was employed to obtain information about the surface morphology and roughness of the polyamide NF membrane. AFM provides high-resolution images of the membrane surface, allowing for the measurement and analysis of surface features at the nanoscale level.

X-ray photoelectron spectroscopy (XPS, Escalab 250Xi, Thermo Fisher Scientific) was utilized to quantitatively analyze the surface element content of the prepared NF membrane. Furthermore, the polyamide cross-linking degree was determined through calculations based on XPS results. XPS is a technique that provides information about the elemental composition and chemical state of the membrane surface.

The charge properties of the membrane surface were determined using a solid surface Zeta potentiometer (SurPASS 3, Anton Paar, Austria). The zeta potential value of the membrane surface was calculated using the Helmholtz–Smoluchowski equation. This measurement was carried out in KCl solution at a temperature of 25 °C. Zeta potential measurements offer insight into the charge distribution and surface electrical properties of the membrane.

The variation of monomer diffusion in the aqueous phase over time was tested using a UV-visible spectrophotometer (UV2800, China). The concentration of PIP in the aqueous phase was characterized by measuring the absorbance at 210 nm. The experiment was conducted at 25 °C.

2.4 Separation performance of membranes

The separation performance of NF membrane was evaluated by cross-flow filtration. And the performance test was carried out at 25 °C and 0.5 MPa. Concentrated water flow was 1.0 L min^{-1}, the pH value was controlled at 6.5–7.0. In order to ensure that the inlet and outlet water reached a steady state during the formal test, the actual water yield by the membrane was collected after 1 h and the single membrane area was 12.5 cm^2. The salt rejection R and the water flux were calculated respectively according to Formula (1) and (2).

$$R = \left(1 - \frac{C_p}{C_r}\right) \times 100\% \quad (1)$$

where R (%) is salt rejection; C_p and C_r are the concentrations of permeate and feed solution, respectively.

$$F = \frac{V}{A \times t} \quad (2)$$

where F (L m^{-2} h^{-1}) is water flux, A (m^2) is the effective membrane area, t (h) is the test time.

3 Results and discussion

3.1 Effect of organic anions and cations on IP process and membrane performance

In terms of molecular structure, the TEAC molecule has a tetrahedral structure with a central nitrogen atom surrounded by four ethyl groups. Due to the presence of quaternary

ammonium salt ions, TEAC molecules display positive charge when dissolved in water. On the other hand, the CSA-Na simultaneously possesses hydrophilic sulfonic acid group and hydrophobic organic ring. Due to the presence of sulfonic acid groups, CSA-Na molecules exhibit negative charge when dissolved in water. According to the principle of similar solubility, the hydrophilic sulfonic acid group was in the aqueous phase and the hydrophobic organic ring was in the organic phase, during the IP process. The positively charged TEAC molecules were attracted to the negatively charged CSA-Na molecules through electrostatic interactions. And they were combined with each other near the water–oil phase interface. This results in the formation of organic combinations near the interface. When reaching a certain concentration, they will be dispersed between the water and oil interfaces. We performed density functional theory calculations using the Gaussian 16 suite, and obtained the farthest distance between atoms in the molecules after molecular optimization at the B3LYP-D3(BJ)/6-31G** level. The calculated farthest distances between atoms for PIP, CSA-Na, and TEAC were 4.56 Å, 7.31 Å, and 6.65 Å, respectively (Fig. 2a). The hypothesis is that these organic structures have the ability to modulate the diffusion of PIP molecules at the molecular level. Consequently, they could greatly occupy the diffusion channel of PIP molecules to the water–oil interface through large volumes and limit the reaction space of IP. As shown in Fig. 2b, the diffusion transport of PIP molecules was confined between combinations of CSA-Na and TEAC. This modulation was believed to significantly impact the diffusion of the PIP monomer to the organic phase and increase the stability of the IP reaction.

To test this hypothesis, we conducted controlled experiments to evaluate the performance of the NF membrane, as depicted in Fig. 2c. The experiments were carried out at a test pressure of 0.5 MPa. In the blank experiment (PA-0), the membrane exhibited a very low flux. However, after introducing CSA-Na and TEAC into the aqueous phase solution, the resulting membrane (PA-CT) showed increased rejection of magnesium sulfate and a significant improvement in flux compared to other membranes.

Specifically, compared to the membrane containing only CSA-Na (PA-C), the membrane with both CSA-Na and TEAC (PA-CT) demonstrated a 32.0% improvement in flux. Similarly, compared to the membrane with only TEAC (PA-T), the membrane with both CSA-Na and TEAC showed a 53.5% improvement in flux. TEAC, with its small molecular free volume and regular structure, is conducive to the increased combination of anionic and cationic organic ions when its concentration is raised.

Additionally, the diffusion behavior of piperazine molecules to the organic phase is affected by the electrostatic repulsion of excess TEAC molecules at the water–oil interface. As a result, in this research, we will further increase the concentration of TEAC in the aqueous phase to explore the optimal concentration ratio of organic anionic and cationic additives.

The UV-vis spectrophotometer was used to investigate the effect of organic ionic additives on the diffusion of PIP

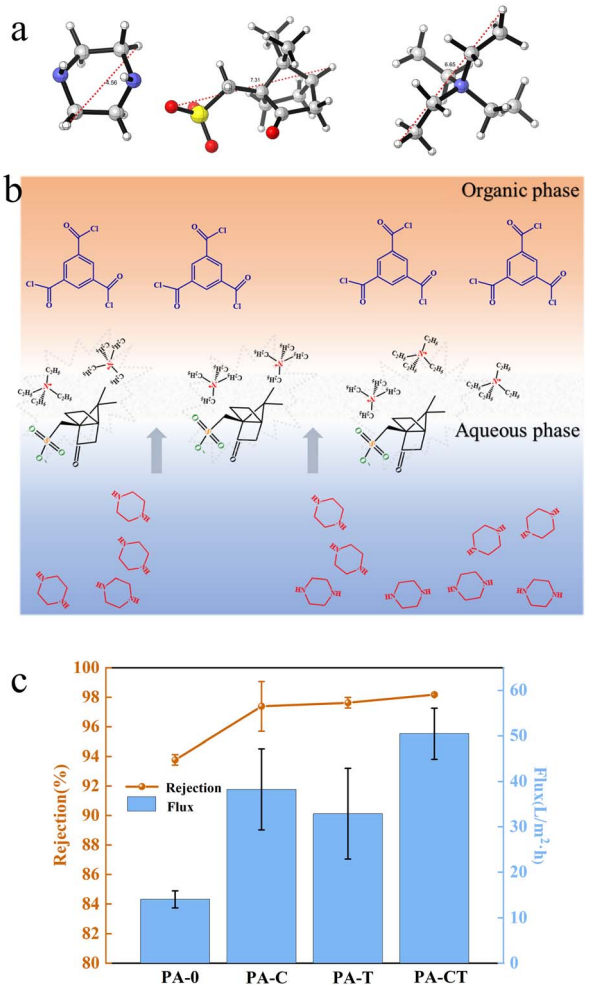

Fig. 2 Schematic diagram of CSA and TEAC modulating PIP diffusion through electrostatic interaction (a), and the farthest distance between atoms in piperazine molecule, camphor sulfonic acid ion and tetraethylammonium ion (b), the effects of adding CSA and TEAC in aqueous phase on the performance of NF membranes (c).

molecules from the aqueous phase to the organic phase (Fig. 3a). The change in concentration of piperazine with time over 300 s was expressed by measuring the absorbance of the aqueous solution. Background interference caused by the introduction of organic ions into the aqueous solution has been removed during the testing process. The absorbance of the blank solution (0%) gradually decreased within 300 s, indicating the progressive diffusion of PIP molecules into the organic phase. However, a notable difference was observed in the absorbance changes when organic ions were added to the aqueous solution, displaying a smoother trend. This could be attributed to the presence of both organic cations and anions provided a smoother and faster diffusion pathway for PIP molecules, which resulted in the completion of diffusion into the organic solvent before the measurement was taken.

3.2 Structural analysis of NF membranes

Firstly, we analyzed the functional groups present in the prepared NF membrane using FTIR. In Fig. 3b, the infrared

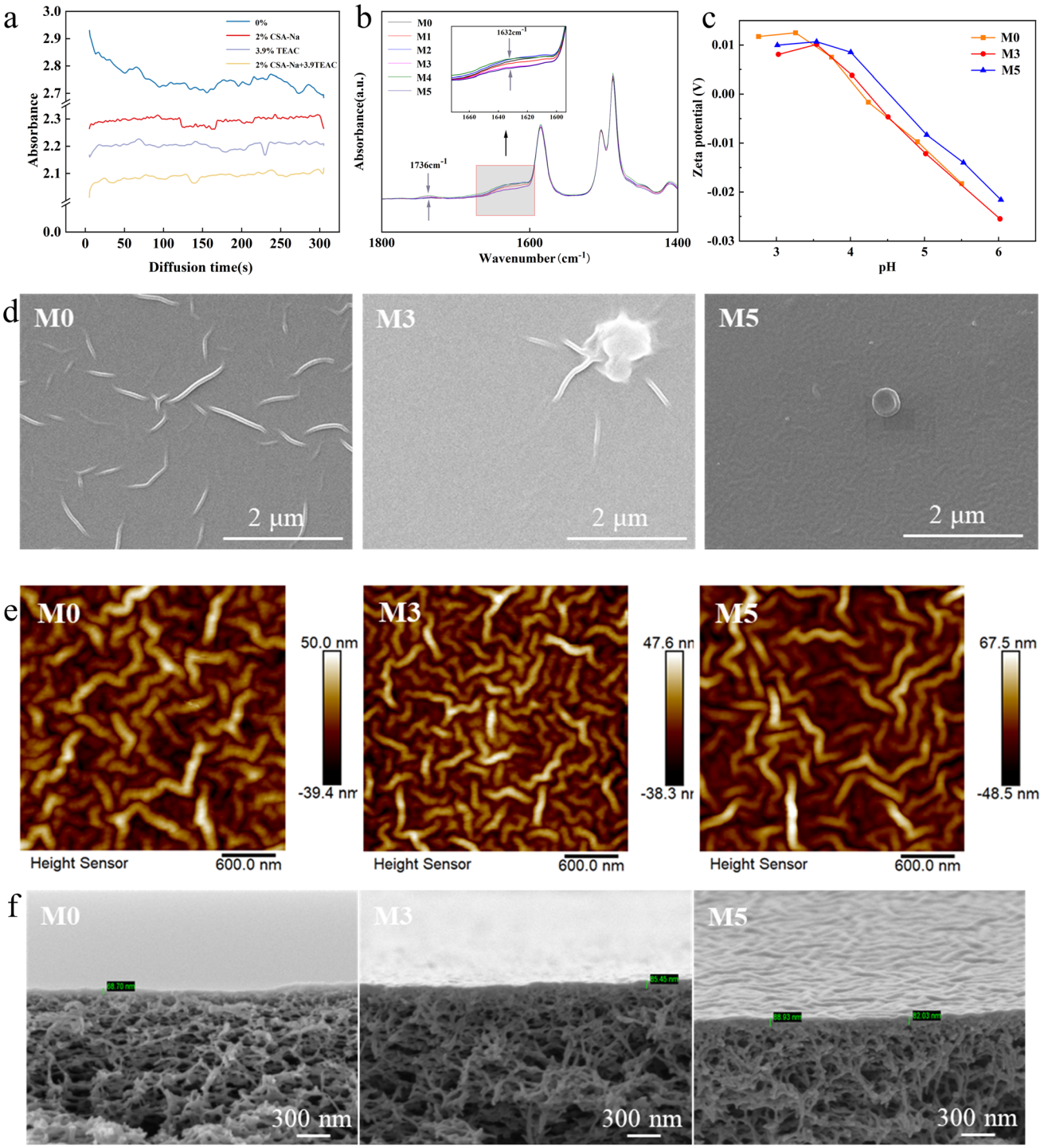

Fig. 3 The change of absorbance of aqueous solution with diffusion time (a) and analysis of morphology and structure of nanofiltration membrane. The FTIR spectra of M0–M5(b), zeta potential of M0, M3, M5 (c), SEM surface images of M0, M3, M5 (d), AFM three-dimensional images of M0, M3, M5 (e). Cross-section SEM images of M0, M3, M5 (f).

spectrum was normalized and the wavenumber range from 1800 cm^{-1} to 1400 cm^{-1} was examined. The addition of PVA in the aqueous phase resulted in a spectral band at 1736 cm^{-1}, corresponding to the ester bond formed between PVA and TMC.[31] The characteristic peak at 1632 cm^{-1} indicated the stretching vibration of the amide group on the C–O bond, confirming the successful formation of the polyamide selective layer.[15] Among the analyzed membranes (M0–M5), the absorption intensity at 1632 cm^{-1} was highest for M2 and M4,moderate for M0 and M1, and lowest for M3 and M5. Compared to M0, no new characteristic peaks were observed in the modified NF membranes.

The elemental composition of the membranes (M0–M5) was quantitatively analyzed using XPS. The degree of membrane cross-linking is often characterized by the O/N element ratio, and a fully cross-linked NF membrane ideally has an O/N value of 1. As shown in Table 2, the overall order of cross-linking degree, from highest to lowest, was M1 = M4 > M2 > M3 > M1 > M5. However, there were only slight fluctuations in the cross-linking degree from M0 to M5. The O/N value for M5 was 1.09, which was close to the value expected for a fully cross-linked PA layer. It is presumed that the addition of TEAC in the aqueous phase reduces surface tension and promotes IP. Among them, M2 and M3 showed a moderate degree of cross-linking. It should be noted that the variation in TEAC content influenced the degree of cross-linking of the composite NF membranes, although the variation was not significant. Additionally, it is worth mentioning that XPS can only detect the elemental composition of the PA layer with a thickness of 1–5 nm (ref. 32) and cannot assess the degree of cross-linking of the entire PA layer. Fig. 3c demonstrates the surface potential characteristics of the composite NF membrane prepared by adding different concentrations of TEAC to the aqueous phase. The zeta potentials of M0, M3, and M5 membranes displayed a noticeable decrease with increasing pH. The positive charge on the membrane surface was attributed to the protonation of the amino group in an acidic environment. Conversely, as the pH increased, the deprotonation of the carboxyl group resulted in a negative charge on the membrane surface. The surface characteristics of the three types of NF membranes were more similar between pH 3.0 and 6.0. The presence of a negative charge on the membrane surface was advantageous for the removal of charged solutes through electrostatic interaction.

Field emission scanning microscopy (FESM) was employed to observe the surface morphology of the NF membrane. The impact of organic anion and organic cation on the physical structure of the membrane is illustrated in Fig. 3d. In the case of M0, the membrane surface exhibited wrinkles and nano-scale particles. Compared with the M0, the membrane of M3 and M5 was without wrinkle-like morphology, with flatter surface. It is hypothesized that the formation of new organic structures near the phase interface greatly occupy the diffusion channel of PIP molecules to the water–oil interface. As TEAC concentrations increase, they are distributed near the interface and PIP diffusion is further inhibited. Since the IP reaction is self-limiting,[33] the inhibited PIP molecules cannot diffuse deeper into the polyamide layer after the IP reaction occurred rapidly to form the nascent film, resulting in the disappearance of the original wrinkled structure.

Table 2 Elemental contents and O/N ratio of the M0–M5

	Atomic concentration (%)			
Membrane	C 1s	N 1s	O 1s	O/N ratio
M0	72.81	12.9	14.3	1.11
M1	74.46	11.72	13.82	1.18
M2	73.71	12.36	13.93	1.13
M3	73.06	12.73	14.21	1.12
M4	72.56	12.6	14.84	1.18
M5	72.91	12.95	14.14	1.09

The surface morphology of the NF membrane as further examined using atomic force microscopy (AFM) (Fig. 3e). As shown in Fig. 3b, the morphologies of the NF membrane were uniformly distributed in the AFM images. The average roughness (Ra)of membrane was 11.7, 11.0, 14.8 nm for M0, M3, M5,respectively. The uniform polyamide layer on the membrane surface was attributed to the mixture of CSA and TEAC, which allowed for the stable diffusion of PIP molecules. In addition, it was observed from cross-sectional SEM images that the thickness of the polyamide layers for M0, M3, and M5 were 68.70 nm, 85.45 nm, and 88.93 nm, respectively (Fig. 3f). The diffusion rate of the amine monomer has an important role in the final thickness of the polyamide layer.[34] The interaction between CSA and TEAC allows PIP molecules to diffuse faster and more uniformly, resulting in an increase in the thickness of the polyamide layer from 68.70 nm to 88.93 nm.

3.3 Performance of NF membrane

3.3.1 Effect of CSA-Na and TEAC in aqueous phase on performance of NF membrane. Water flux and rejection are important indicators for evaluating the separation performance of NF membranes. In Fig. 4a, the water flux of M0 was measured as 37.70 L m^{-2} h^{-1} at a test pressure of 0.5 MPa, with a high rejection of 98.3% for $MgSO_4$. With the increase in TEAC concentration, the water flux of the membrane increased from 37.70 L m^{-2} h^{-1} to 55.61 L m^{-2} h^{-1}, while maintaining over 98% rejection for $MgSO_4$ in M1 to M3. This enhancement can be attributed to the formation of larger organic structures by the addition of CSA-Na and TEAC in the aqueous phase, effectively blocking the diffusion of monomers. Increasing the TEAC content created narrower molecular diffusion channels at the water–organic interface, restricting the interphase transport behavior of monomers. After the reaction, the separation layer became thinner, and the formed granular convex structures provided additional water molecular channels.

When comparing with the performance of the membranes containing only CSA-Na (PA-C) and only TEAC (PA-T), the water fluxes were 38.24 L m^{-2} h^{-1} and 32.90 L m^{-2} h^{-1} (at a test pressure of 0.5 MPa), respectively. The water flux significantly improved when CSA-Na and TEAC were mixed in the aqueous solution. The optimal concentration ratio of anion and cation mixing was explored by adjusting the TEAC content in the aqueous phase. The results showed that when the CSA-Na content was 2% w/v and the TEAC content was 3.9% w/v (with a ratio of 1 : 3), the water flux reached the maximum value of 55.61 L m^{-2} h^{-1}.

To investigate the separation selectivity of the NF membranes, $MgSO_4$ and NaCl were chosen as representative inorganic salts. As shown in Fig. 4b, the rejection of $MgSO_4$ by the composite NF membrane was significantly higher than that of NaCl. This can be attributed to the combined effects of the Dornan rejection effect and the pore size sieving effect.[35–37] The negatively charged surface of the TFC membrane in this study led to its repulsion of similarly charged negative ions, while

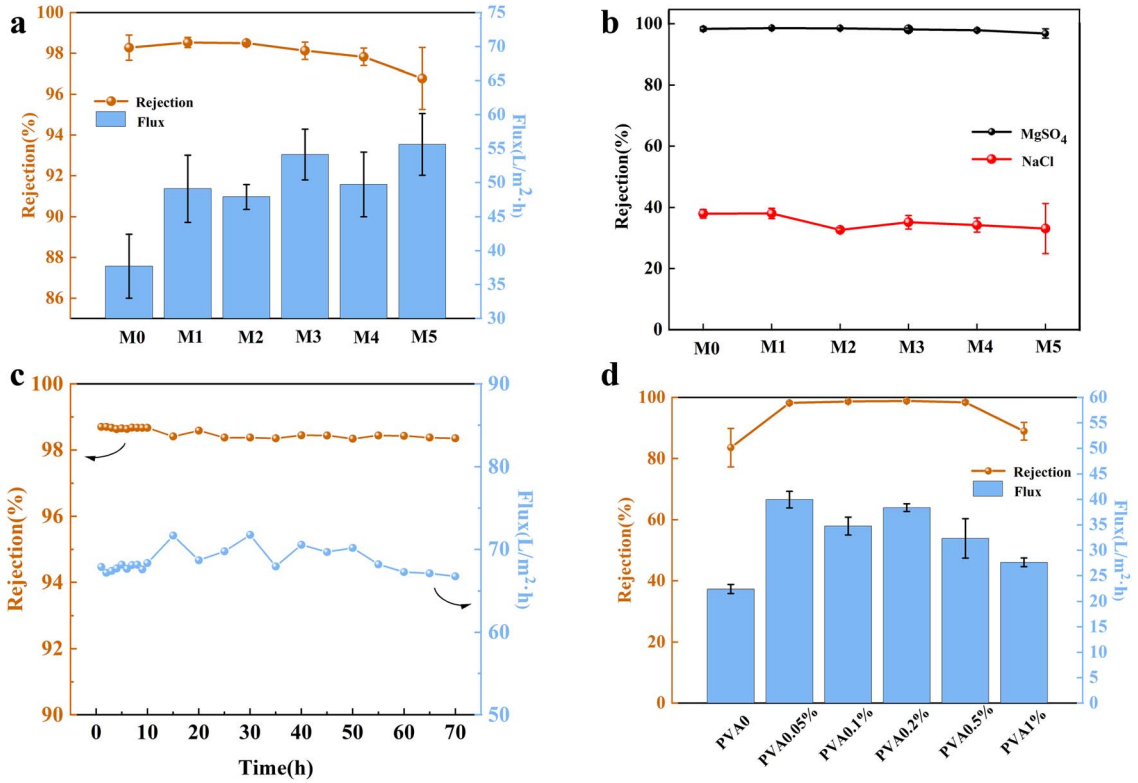

Fig. 4 Performance of NF membrane. Water flux and $MgSO_4$ rejection of NF membranes (a), salt rejection properties of NF membranes (b) long-term stability of the M3 (c), the effect of different content of PVA on the properties of the membrane (d).

attracting positively charged ions into the membrane. This resulted in a higher concentration of positively charged ions inside the membrane compared to the feed solution, maintaining electrical neutrality and inhibiting the migration of positively charged ions to the membrane's inner side, known as the Dornan repulsion effect. The higher the valence of the same charge ion, the stronger the repulsion effect,[38] hence the higher rejection of SO_4^{2-} compared to Cl^-. Furthermore, Cl^- has a smaller hydration radius and larger diffusion coefficient than SO_4^{2-},[26] making it easier for Cl^- to pass through the membrane. Thus, considering the charge effect and pore size characteristics of the NF membrane, it exhibits distinct advantages in the field of mono/divalent ion separation.

In addition, the long-term test was carried out under the pressure of 0.5 MPa and the feed solution of 2000 ppm $MgSO_4$ solution. The M3 exhibited desirable $MgSO_4$ rejection with slight flux changes for 70 h (Fig. 4c).

3.3.2 Effect of PVA in aqueous phase on performance of NF membrane. Furthermore, we hope to regulate the diffusion of PIP effectively by introducing PVA into the aqueous solution. The effect of additional addition of PVA to the aqueous phase on the film properties was investigated. For a fixed CSA-Na content of 2% w/v and TEAC content of 3.9% w/v in the aqueous phase, we examined the effect of increasing PVA content from 0% w/v to 1% w/v on the performance of the NF membrane. Fig. 4d illustrates the separation performance of the prepared composite NF membrane. As the PVA content increased from 0.0% w/v to 0.05% w/v, the water flux increased from 22.4 L m^{-2} h^{-1} to 40.0 L m^{-2} h^{-1} (at a test pressure of 0.5 MPa), while the rejection of $MgSO_4$ increased from 83.6% to 98.2%. However, when the PVA content exceeded 0.2% w/v in the aqueous phase, the membrane performance started to decrease significantly.

Compared to PVA content of 0.05%, the membrane with PVA content of 0.1% exhibits higher rejection. This resulted in a slight decrease in its water flux. Therefore, it can be concluded that the prepared composite NF membrane exhibited superior separation performance when a low concentration of PVA and organic ions coexisted. The introduction of PVA effectively improved the solution viscosity and the chain-like polymer of PVA significantly increased the diffusion resistance of the PIP monomers during the interfacial polymerization.[31] In solution, PVA can inhibit the diffusion rate of PIP monomer; at the phase interface, the organic structure created by CSA-Na and TEAC can modulate the transport behavior of PIP monomer. In summary, we created a suitable environment for the diffusive transport of the monomer in the aqueous phase solution.

4 Conclusions

In conclusion, through the manipulation of the IP process using CSA-Na and TEAC as additives in the aqueous phase, we successfully obtained NF membranes with excellent separation performance. The electrostatic interaction between CSA-Na and TEAC played a crucial role in constraining the transport behavior of PIP at the phase interface. With the combination of

CSA and TEAC, numerous larger organic combinations were formed. They partially occupied the diffusion channel of PIP molecules to the oil phase, thus significantly affecting the diffusion of piperazine to the water–oil phase interface. Specifically, when the CSA-Na content was 2% w/v, TEAC content was 3.9% w/v, and the ratio of the amount of substance between them was 1 : 3, the resulting NF membranes exhibited the highest permeate flux while rejection of $MgSO_4$ was 98%. Importantly, the introduction of additional organic ions in the aqueous phase did not destabilize the interface, but rather effectively modulated the diffusion behavior of the monomers at appropriate concentrations. This study provides valuable insights into the creation of a favorable diffusive transport environment for monomers and offers new perspectives for further exploration in this field.

Author contributions

Zhou Shuai: methodology, investigation, formal analysis and writing; Tan Huifen: methodology, conceptualization, project administration and validation Chen keke: methodology, conceptualization, visualization; Cheng Xin: methodology, conceptualization; Huang xiaojuan: data curation; Gao congjie: resources.

Conflicts of interest

There are no conflicts to declare.

Acknowledgements

This work was supported by the National Key Research and Development Program of China (No. 2021YFB3801100); the Key research and Development Project of Zhejiang Province (No. 2021C01173) and Zhejiang Key Laboratory of Seawater Desalination Technology Research (No. 2012E10001).

Notes and references

1 M. A. Shannon, P. W. Bonn, M. Elimelech, J. G. Georgiadis, B. J. Marinas and A. M. Mayes, *Nature*, 2008, **452**, 301–310.
2 M. Elimelech and W. A. Phillip, *Science*, 2011, **333**, 712–717.
3 P. Marchetti, M. F. Jimenez Solomon, G. Szekely and A. G. Livingston, *Chem. Rev.*, 2014, **114**, 10735–10806.
4 P. Vandezande, L. M. Gevers and I. J. Vankelecom, *Chem. Soc. Rev.*, 2008, **37**, 365–405.
5 M. Buonomenna, *Sep. Purif. Rev.*, 2015, **44**, 157–182.
6 J. C. Jose Torres, M. A. Ochoa and N. Pagliero, *Process Saf. Environ. Prot.*, 2021, **148**, 825–833.
7 W. Zhang and X. Zhang, *J. Membr. Sci.*, 2021, **632**, 119358.
8 M. B. M. Y. Ang, Y.-T. Lu, S.-H. Huang, J. C. Millare, H.-A. Tsai and K.-R. Lee, *J. Polym. Res.*, 2022, **29**, 90–99.
9 Z. Wang, S. Liang, Y. Kang, W. Zhao, Y. Xia, J. Yang, H. Wang and X. Zhang, *Prog. Polym. Sci.*, 2021, **122**, 101450.
10 C. Ji, Z. Zhai, C. Jiang, P. Hu and Q. J. Niu, *Desalination*, 2020, **500**, 114869.
11 Z. Wang, S. Liang, Y. Kang, W. Zhao and X. Zhang, *Prog. Polym. Sci.*, 2021, **122**, 101450.
12 A. P. Korikov, P. B. Kosaraju and K. K. Sirkar, *J. Membr. Sci.*, 2006, **279**, 588–600.
13 K. Yoon, B. S. Hsiao and B. Chu, *J. Membr. Sci.*, 2009, **326**, 484–492.
14 A. L. Ahmad, B. S. Ooi and J. P. Choudhury, *Desalination*, 2003, **158**, 101–108.
15 S. M. Kim, S. Hong, B. Nguyen, H. Thi, S. H. Park and J. F. Kim, *Polymers*, 2021, **13**, 1716.
16 L. Xu, W. Zhi, B. Xha, B. Yla, W. Chong, B. Fya and B. Jwa, *J. Membr. Sci.*, 2021, **640**, 119765.
17 M. Solomon, Y. Bhole and A. G. Livingston, *J. Membr. Sci.*, 2013, **434**, 193–203.
18 Y. Zhao, Z. Zhang, D. Lei, H. Mao and S. Zhang, *J. Membr. Sci.*, 2017, **522**, 175–182.
19 A. P. Rao, N. V. Desai and R. Rangarajan, *J. Membr. Sci.*, 1997, **124**, 263–272.
20 H. Dong, L. Zhao, L. Zhang, H. Chen, C. Gao and W. W. Ho, *J. Membr. Sci.*, 2015, **476**, 373–383.
21 M. You, B. Wang, L. An, F. Xu and J. Meng, *Chem. Eng. Res. Des.*, 2021, **165**, 1–11.
22 Z. Yao, G. Hao, Y. Zhe, Q. Weihua and C. Y. Tang, *Desalination*, 2018, **445**, 115–122.
23 J. Yin and B. Deng, *J. Membr. Sci.*, 2015, **479**, 256–275.
24 J. H. Jhaveri and Z. Murthy, *Desalination*, 2016, **379**, 137–154.
25 X. Li, A. Sotto, J. Li and V. Bart, *J. Membr. Sci.*, 2017, **524**, 502–528.
26 S. Wei, Y. Chen, X. Hu, C. Wang, X. Huang, D. Liu and Y. Zhang, *J. Taiwan Inst. Chem. Eng.*, 2020, **112**, 169–179.
27 S. F. c. Z. Tan, X. S. Peng, L. Zhang and C. J. Gao, *Science*, 2018, **360**, 518–521.
28 Y. Sun, W. Jin, L. Zhang, N. Zhang, B. Wang and B. Jiang, *J. Appl. Polym. Sci.*, 2018, **135**, 46363.
29 C. Y. Zhu, C. Liu, J. Yang, B. B. Guo and Z. K. Xu, *J. Membr. Sci.*, 2021, **627**, 119142.
30 Q. Zhang, Y. Wang, Y. Zhao, C. Ma, X. Xu, W. Gu, Y. Yang and S. Wang, *Chinese J. Org. Chem.*, 2019, **39**, 2616–2624.
31 S. Zhao, S. Xue, L. Li, C. Ji, P. Li and Q. J. Niu, *Colloids Surf. A: Physicochem. Eng. Asp.*, 2023, **660**, 130870.
32 M. Morgenstern, T. Strasser, R. Adelung, M. Getzlaff and L. Kipp, *Phys. Rev. B: Condens. Matter Mater. Phys.*, 2004, **70**, 81305.
33 J. S. Maqsud, R. Chowdhury, B. D. Huey and J. R. McCutcheon, *Science*, 2018, **361**, 682–686.
34 M. Zhang, X. You, K. Xiao, Z. Yin, J. Yuan, J. Zhao, C. Yang, R. Zhang, H. Wu and Z. Jiang, *J. Membr. Sci.*, 2022, **657**, 120673–120680.
35 Y. Zhang, J. Guo, H. Gang, Y. Bai and L. Shao, *Sci. Adv.*, 2021, **7**, 8706.
36 C. Yang, Y. Li, M. Long, P. Yang, Y. Li, Y. Zheng, R. Zhang, Y. Su, H. Wu and Z. Jiang, *J. Membr. Sci.*, 2022, **642**, 119944.
37 Z. Thong, G. Han, Y. Cui, J. Gao, T. S. Chung, S. Y. Chan and S. Wei, *Environ. Sci. Technol.*, 2014, **48**, 13880–13887.
38 J. Sabaté, J. Labanda and J. Llorens, *J. Membr. Sci.*, 2009, **345**, 298–304.